Proximity-Effect Superconductive Tunneling in Nb on InGaAs/InP/InGaAs Heterostructures

A. Kastalsky, L. H. Greene, J. B. Barner, and R. Bhat
Bellcore, 331 Newman Springs Road, Red Bank, New Jersey 07701
(Received 6 November 1989)

We present experimental data on proximity tunneling in InGaAs/InP/InGaAs heterostructures due to a Nb film which induces superconductivity in the top InGaAs layer. The proximity effect is demonstrated in tunneling measurements yielding superconducting parameters induced in the top InGaAs layer, such as the gap, Δ, the tunneling density of states, $D(E)$, and their variations with the temperature, T. We observe a significant smearing of $D(E)$. This is attributed to a spatial decay of the gap into the depth of the InGaAs layer. Superconductivity in InGaAs is also directly evidenced through measurements of the lateral current using a sequence of Au-Nb-Au pads on InGaAs.

PACS numbers: 74.50.+r, 73.40.Gk, 73.40.Qv, 73.40.Ty

Recent studies of the proximity effect in semiconductors, such as Si, InAs, InGaAs, and GaAs, have demonstrated success in the Cooper tunneling through the surface and/or Schottky barriers and in the proximity-induced superconductivity in semiconductors.[1] Coherence lengths as large as 3000 Å have been observed in InAs layers.[2] InGaAs has proven to be a promising material,[3] since it has a low Schottky-barrier height ($\sim$0.2 eV), and heavy doping ($\sim 10^{19}$ cm^{-3}) in the top portion of this layer makes the Schottky barrier more permeable for Cooper pairs. These previous investigations[1] were motivated by the search for a superconducting field-effect transistor wherein results were interpreted in terms of coherence lengths.

Tunneling is known to be the most sensitive probe of the superconducting state, yielding such important parameters as the gap, electron density of states, phonon spectra, etc.[4] Tunneling into normal-metal–superconductor (NS) sandwiches has been extensively used for studying proximity effects in metal-based SNIN structures (I denotes insulator).[5] In our experiment, we apply the same method of SNIN tunneling to a semiconductor, NIN-like heterostructure in which the electron effective masses, m^*, and Fermi velocities, v_F, are about 20 times, and the densities, n, are about 10^6 times, lower than in the metal. The well-advanced semiconductor heterostructure technology allows preparation of high-quality barriers of required thickness, shape, and height which makes the tunneling experiments reproducible and reliable. Furthermore, the precise control of layer doping allows the fabrication of markedly thinned Schottky barriers for efficient Cooper-pair transport into the semiconductor. We report here, for the first time, a successful realization of superconductive tunneling in the SNIN structure in which the NIN part is an InGaAs/InP/InGaAs heterostructure.

Semiconductor heterostructures are grown by organo-metallic-chemical-vapor deposition. Subsequently, a 2000-Å Nb film is dc-sputter deposited at ambient temperature after surface cleaning in a 1:20 NH_3OH:H_2O solution. Patterning of the structure to obtain junction areas of 20×20 μm^2 is accomplished by standard photolithographic techniques. The critical temperature of the Nb film, obtained by four-probe measurements of the lateral resistance, yields $T_c = 9.2$ K.

The inset to Fig. 1 shows the basic tunneling structure. It comprises a 100-Å-thick InP insulating barrier sandwiched by two lattice-matched $In_{0.53}Ga_{0.47}As$ layers, each with electron density $n = 3\times10^{17}$ cm^{-3}. The top 100 Å of the InGaAs layer with $n\sim1\times10^{19}$ cm^{-3} serves (as discussed above) to reduce the Schottky-barrier width. Two different thicknesses of the top InGaAs layer, $d = 1000$ and 3000 Å, are grown so that the thickness dependence of the proximity effect can be investigated. The graded 500-Å n^+ $InGa_{1-x}P_xAs$ layer is used to minimize a barrier between the tunneling structure and the n^+ InP substrate.

The dynamic resistance, $R(V) = dV/dI(V)$, of our structure, which was acquired by current-biased, low-frequency ($\sim$500 Hz) lock-in techniques, is shown in Fig. 1 for $T = 4.2$ K. The voltage, V, and the applied current, I, are measured between the Nb and substrate in a four-probe configuration. Two distinct features are observed. The first is a superconducting-gap structure ($\sim$1 mV) with a peak of $\sim$11 kΩ. This gap feature is absent at 8 K (dashed curve). The second is oscillations, extending out to a few hundred mV, which are due to ballistic electron motion across the InGaAs layers.[6] The period of oscillation (15–30 mV depending upon the bias, V) agrees reasonably well with the energy values for the excited levels in the 1000-Å InGaAs quantum well. Thus, we obtain an intriguing combination of both superconducting and semiconducting properties in the same structure. At the lowest temperature of the experiment, $T = 1.2$ K, the superconducting-gap feature dominates the junction resistance, yielding $R(0) = 330$ kΩ and a resistance ratio of $R(0)/R(1.5\text{ mV})\sim220$, which is indicative of a low-leakage, high-quality barrier. The corresponding I-V characteristics for different temperatures are shown in the right inset to Fig. 1. The critical temperature, determined by the disappearance of the gap, is $T_c = 7.55\pm0.05$ K, which is lower than that of

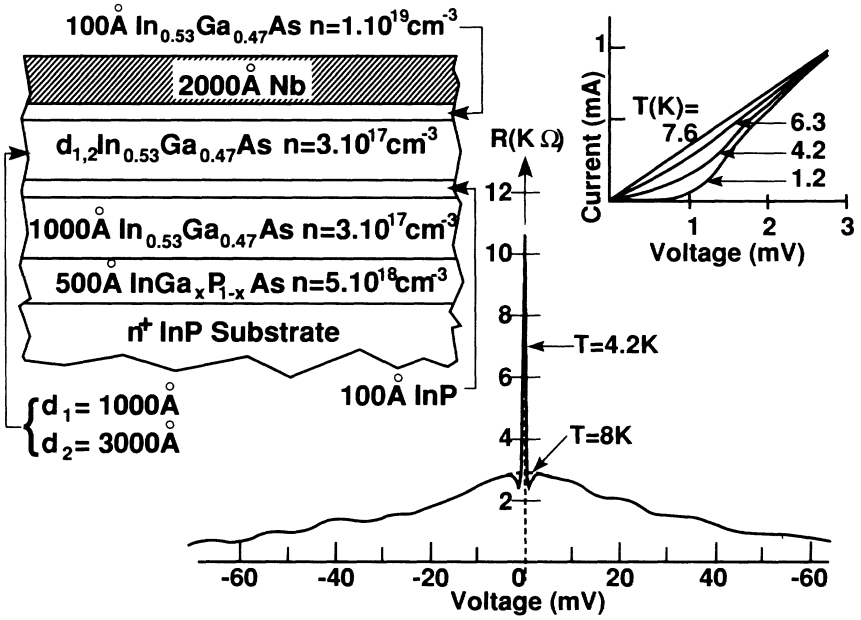

FIG. 1. Dynamic resistance, $R=dV/dI$, as a function of voltage for $T=4.2$ and 8 K for the tunneling structure which is schematically drawn in the left inset. Here, $d=1000$ Å. Right inset: I-V characteristics for several temperatures.

bulk Nb.

From this dynamic resistance, the dynamic conductance, $\sigma(V)/\sigma_n$, where σ_n is the normal-state conductance, is obtained and compared with the semiclassical model:[7]

$$\frac{\sigma(V)}{\sigma_n}=\int_{-\infty}^{\infty}\frac{D(E)}{D(0)}\left[\frac{\partial f(E+eV)}{\partial(eV)}\right]dE\,, \tag{1}$$

where $f(E)$ is the Fermi distribution function and $D(E)$ is the BCS density of states, i.e.,

$$D(E)=\begin{cases}0 \text{ for } |E|<\Delta\,,\\ D(0)\dfrac{E}{(E^2-\Delta^2)^{1/2}} \text{ for } |E|>\Delta\,.\end{cases}$$

Throughout all of these calculations, we have used a temperature-dependent gap,[8] $\Delta(T)$. In Fig. 2 the experimentally obtained $\sigma(V)/\sigma_n$ is shown together with the curves calculated from Eq. (1). We emphasize the similarity of these curves, although the electronic properties of the normal states of metals and semiconductors are vastly different. To take into account that the experimental curve is broadened, in the calculation we redefine Δ by entering a phenomenological parameter α,

$$\Delta'=\Delta+i\alpha\Delta\,, \tag{2}$$

and this expression is used in Eq. (1) for further analysis. This approach is equivalent to smearing the gap uniformly as a function of energy for the entire energy range. A high value of $\alpha=0.10$ is required to obtain the best fit, yielding $\Delta=1.29$ meV (for $T=0$). Note that this derived gap value is lower than that for pure Nb ($\Delta_{Nb}=1.52$ meV, Ref. 9). However, using the measured $T_c=7.55$ K, the ratio $2\Delta/k_BT_c$ remains at 3.97 ± 0.05, which is close to that of Nb (3.89, Ref. 9).

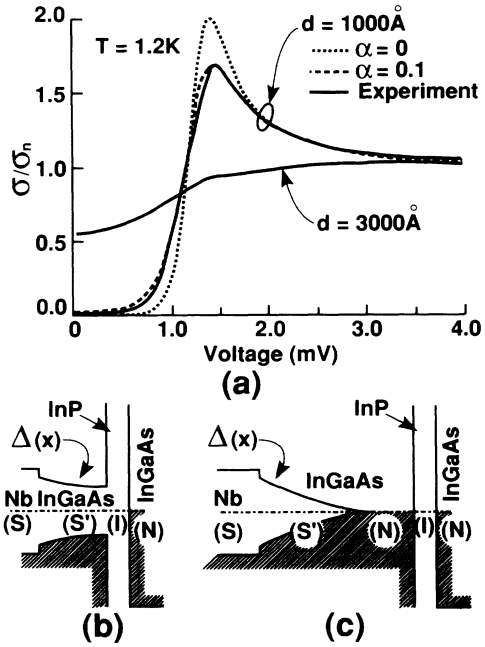

FIG. 2. (a) The normalized conductance as a function of voltage for 1.2 K for two different proximity-layer thicknesses. For the case of $d=1000$ Å, the experimental data together with two theoretical curves for $\alpha=0$ and 0.1, both using $\Delta=1.29$ meV, are presented. For the case of $d=3000$ Å, only the data are presented, as discussed in the text. Proposed energy-band diagrams of our structures for (b) $d=1000$ Å and (c) $d=3000$ Å are shown.

The physical origin of the smearing is not completely understood. We do not believe quasiparticle lifetime effects are responsible for such a dramatic broadening. A position-dependent gap parameter which decreases from its value at the Nb interface into the bulk of InGaAs [as illustrated schematically in Fig. 2(b)] could play the most significant role. As a result of this spatial variation, the peak of the density of states is expected to be broadened: As the voltage is increased, the electrons tunneling through the InP barrier and moving through the InGaAs top layer experience different energy gaps. In this case, the value of $\Delta = 1.29$ meV could be considered as a mean value within this energy interval.

The dependence $\sigma(V)/\sigma_n$ for the sample with $d = 3000$ Å is also presented in Fig. 2. One can see a severe broadening of this curve as well as a high zero-bias conductance. As in the previous case, we attribute this result to the gap decreasing towards the barrier. Even at the lowest temperature, 1.2 K, it would appear that a significant portion of the InGaAs remains gapless, as shown in Fig. 2(c). This would give rise to a nonsuperconducting component, dominating the tunneling current at low bias. Note also in the conductance data of Fig. 2 the rise in conductance above 1.3 mV. This feature could be attributed to the appearance of a bound state in the superconducting part of InGaAs. More experimental work is needed in order to determine the origin of this structure. We have been unable to fit the conductance data for the $d = 3000$ Å structure at any α. Finally, we emphasize that the obtained striking difference in Fig. 2 for the two structures discussed is strong evidence for the occurrence of superconductive tunneling [SS'IN, see Fig. 2(b)] in the InGaAs/InP/InGaAs as opposed to the Nb/Schottky-barrier/InGaAs tunneling.

The temperature dependences of the normalized zero-bias conductances, $\sigma(0)/\sigma_n$, of our two structures are shown in Fig. 3. We have fitted the data for the $d = 1000$ Å structure using a temperature dependence of $\Delta(T)$ in Eqs. (1) and (2), and coupling constant $2\Delta/k_B T_c = 3.97$. Considering our rather simple approach with two adjustable parameters, α and Δ, the fit seems reasonable. Thus, using these parameters, both $\sigma(V)/\sigma_n$ and the temperature dependence of $\sigma(0)/\sigma_n$ were fitted.

For the sample with the $d = 3000$ Å proximity layer, we observe a weak temperature dependence for $\sigma(0)/\sigma_n$ and saturation at low temperatures. This contrasts with the behavior of conventional SIN junctions which exhibits a strong drop in zero-bias conductance with decreasing temperature.[9] It is also interesting to note that the drop in the zero-bias conduction starts at the same temperature as in the 1000-Å proximity-layer sample, ~7.5 K. One can suggest that this feature originates from the superconducting part of the InGaAs layer, closest to the Nb interface. The small fraction of electrons tunneling through the InP layer and moving ballistically through the InGaAs proximity layer experiences normal reflections and returns back, thereby reducing the total conductance. At low temperatures the gap increases and the number of electrons involved in this reflection process (within $\sim 2k_B T$) rises, contributing to the resistance. A further temperature decrease leads to stabilization of this process and a conductance saturation. Thus, the proposed picture, because it contains a normal portion in the top InGaAs layer, is distant from the conventional mechanisms for SIN tunneling. This is why our fits for the 3000-Å proximity layer have failed at any α.

Besides the thickness dependence of the proximity layer on superconducting properties, we present here further evidence of the superconductivity induced in the InGaAs through the Schottky barrier. Experiments on a differently designed semiconductor-superconductor structure were performed. In this case we measure a *lateral* conductance *along* the top InGaAs layer by using two gold contacts deposited 0.5 μm from a Nb pad, as

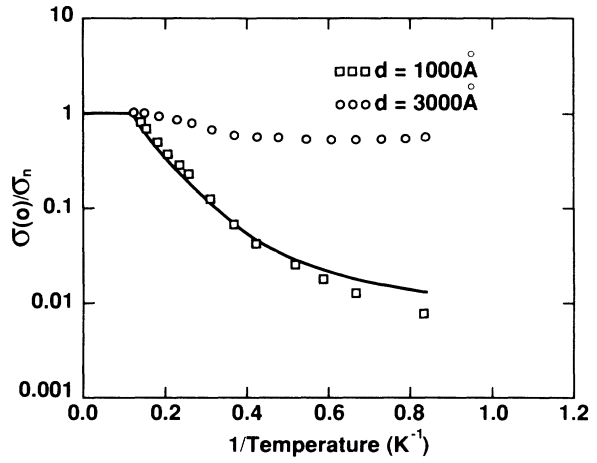

FIG. 3. The zero-bias normalized conductances as a function of temperature for the two proximity-layer thicknesses investigated.

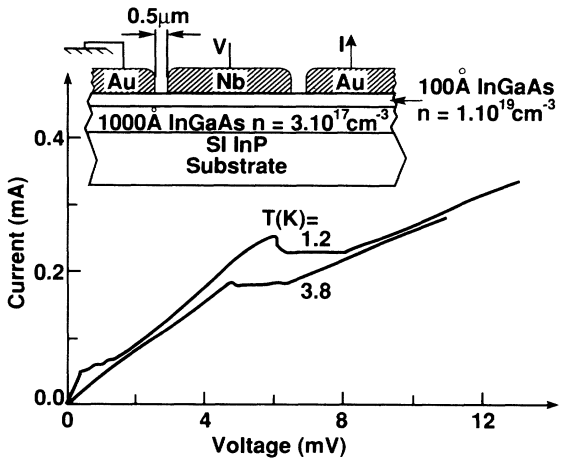

FIG. 4. The I-V characteristics for $T = 1.2$ and 3.8 K for the lateral measurements on the structure in the inset. Note the switching behavior at $I = 0.05$ mA and ~0.2 mA.

shown in the inset of Fig. 4, and we believe that the following interpretation best describes the following data. The I-V characteristic at $T=1.2$ K is shown in Fig. 4. When current is driven between the two gold contacts, it flows in series through normal and superconducting regions of the 0.5-μm-long InGaAs channel between the Au and Nb pads as well as laterally along the Nb/InGaAs (S-S') sandwich. When the Nb (and InGaAs underneath) are superconducting, a voltage drop between the Au and Nb pads appears only across the normal part of the 0.5-μm-long InGaAs layer. A smooth transition to a higher resistance at $I > 50$ μA is due to the gradual removal of the supercurrent in the superconducting region of this 0.5-μm-long InGaAs channel. At higher bias, another transition is observed as a sharp switch due to the removal of superconductivity in the S-S' Nb/InGaAs sandwich. The measured lateral critical current for this sandwich is $\sim 10^4$ A/cm^2. At $T=3.8$ K the proximity-induced feature is less pronounced. Thus, the data shown in Fig. 4 are in accord with the model of proximity-induced superconductivity in the InGaAs layer.

In conclusion, we have demonstrated for the first time, SNIN tunneling in Nb/InGaAs/InP/InGaAs where the layer of InGaAs in contact with the Nb is superconducting through a weakened Schottky barrier by the proximity effect. The proximity effect in InGaAs/Nb was also directly evidenced in a separate experiment of lateral geometry. The observed proximity effect shows a dramatic InGaAs thickness dependence. For a proximity layer of 1000 Å, we have fitted a simple model for the density of states and the temperature dependence of the conductance using two adjustable parameters to take into account the observed broadening. The latter, in our view, comes from a spatially varying gap which decays from the surface to the tunneling barrier. A gap value of $\Delta=1.29$ meV for the Nb/1000-Å-InGaAs proximity layer was derived from the fit.

It is a pleasure to thank W. L. Feldmann for technical support and J. M. Rowell, C. T. Rogers, R. F. Leheny, and J. H. Wernick for scientific discussions.

[1]See, for example, A. W. Kleinsasser and W. J. Gallagher, in *Modern Superconducting Devices,* edited by P. Rudman and S. Ruggiero (Academic, Boston, 1989), and references therein.

[2]H. Takayanagi and T. Kawakani, in *Proceedings of the International Electron Device Meeting* (IEEE, New York, 1985), p. 98.

[3]A. W. Kleinsasser, T. N. Jackson, D. McInruff, G. D. Pettit, F. Rammo, B. Bumble, and J. M. Woodall, Appl. Phys. Lett. **55**, 18 (1989).

[4]J. M. Rowell, in *Tunneling Phenomena in Solids,* edited by E. Burstein and S. Lundqvist (Plenum, New York, 1969), p. 385.

[5]See, for example, E. L. Wolf, and G. B. Arnold, Phys. Rep. **91**, 31 (1982), and references therein.

[6]See, for example, K. K. Choi, P. G. Neuman, P. A. Folkes, and G. J. Iafrate, Appl. Phys. Lett. **54**, 359 (1989); and P. England, J. R. Hayes, M. Helm, J. P. Harbison, L. T. Florez, and S. J. Allen, Jr., Appl. Phys. Lett. **54**, 1469 (1989).

[7]M. Tinkham, *Introduction to Superconductivity* (McGraw-Hill, New York, 1975), p. 43.

[8]C. Kittel, *Introduction to Solid State Physics* (Wiley, New York, 1976), 5th ed., p. 367.

[9]E. L. Wolf, *Principles of Electron Tunneling Spectroscopy* (Oxford Univ. Press, London, 1985), p. 527.